Computational Analysis of Unidirectional Hybrid Composite Materials

Pedro de Herédia de Almeida
pedro.heredia@tecnico.ulisboa.pt

Instituto Superior Técnico, Universidade de Lisboa, Portugal

November 2018

Abstract

The objective of this work is to develop a finite element model to study the behaviour of unidirectional composites, hybrid and non-hybrid, when subjected to longitudinal loads. The study of the hybridization aims the achievement of pseudo-ductility in composite materials. In order to represent with more precision the material microstructure, a new method to obtain the geometry of the transverse section of a representative volume element with a random distribution of fibres in the matrix is presented. The problem is approached as an optimization problem and solved with the help of a genetic algorithm, and the method is able to achieve high levels of fibre volume fraction. The study of homogenization was briefly discussed and it is concluded that for randomly arranged fibres there is a substantial gain on the material properties when compared to a regular fibre packing. Finally, the damage model for the microstructure is implemented imposing strains in the longitudinal direction of the fibres. The fibre failure is gradual so that the stress-strain curve obtained is more detailed. Results are studied for two non-hybrid composites reinforced with distinct carbon fibres and the resulting hybridization of the two types of fibres. The results show that the influence of fibre tensile strength distribution in the mechanical behaviour of the material prevails over the influence of the microstructure geometry. The studied hybrid composite demonstrates tendency to achieve a pseudo-ductile behaviour, but this less drastic development of the failure of the microstructure causes a clear decrease in the material strength.

Keywords: Unidirectional composites, Hybridization, Randomness in fibre distribution, Homogenization, Pseudo-ductility

1. Introduction

Modelling the random fibre distribution of a fibre-reinforced composite is of great importance when studying the progressive failure behaviour of the material on the micro-scale. Most of the existing methods regard the micro-scale geometry as a periodic structure, assuming a deterministic and ordered distribution of fibres. However, the realistic distribution of fibres has been known to be non-uniform and randomly distributed. Therefore, methods based on periodic fibre distributions cannot give accurate predictions of the effective properties of the composite. Wongsto and Li [1] compared the mechanical properties obtained for random and periodic distributions and concluded that the Young and shear moduli from UD composites have higher values for a random packing.

The tensile failure of UD composites is a drastic process due to the propagation of clusters of broken fibres and hybridization can change this behaviour by changing the failure mechanisms in composite materials. Usually composite materials undergo catastrophic failure with a stress-strain diagram as presented in Figure 1(a). Hybridizing the composite material changes the failure process which results in stress-strain diagrams similar to Figure 1(b), where the two load drops correspond, respectively, to the failure of the LE fibres and the HE fibres. By understanding the controlling factors in the behaviour of hybrid composite materials it is possible to design a material with a pseudo-ductile behaviour, as illustrated in Figure 1(c).

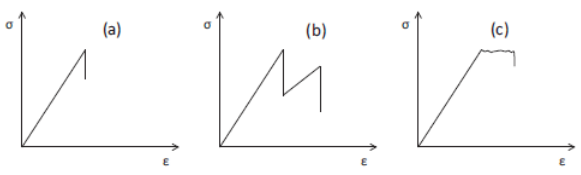

Figure 1: Schematic stress-strain diagrams for (a) non-hybrid composites, (b) typical hybrid composites, and (c) pseudo-ductile hybrid composites [2].

A gradual failure of the composite allows its iden-

tification before the material looses its structural integrity. Thus, a lot of effort is being made regarding the prediction of tensile failure of UD composites and their hybrid behaviour. Turon et al. [3] developed a progressive damage model based on fibre fragmentation, which was extended by Tavares et al. [4] for the study of hybrid composites. In this later article, a dry tow model was also developed to predict the effects of fibre hybridization without matrix concerns, and additionally a micromechanical model taking into account the more complex mechanisms such as the damage in the matrix, fibres and interface. Conde et al. [5] used both the dry tow and the progressive damage model to optimize the material properties for the closest pseudo-ductile stress-strain curve. Tavares et al. [6] applied the spring element model (SEM) proposed by Okabe et al. [7] with periodic packings with random hybrid fibre packings. The model was created as an alternative to 3D FEM to provide low computational cost. The SEM is based on the assembly of periodic packages of fibre and matrix spring elements and takes into account local stress redistribution due to fibre failure. However, in spite of the computational effort 3D FEM provide more accuracy and can portray better the reality by providing continuous mesh surfaces and volumes connecting fibres and matrix. The objective of this work is to develop a three-dimensional micromechanical damage model to predict the tensile failure of UD composites and take into account the possibility of hybridization. The goal is to provide a tool than can study the composite behaviour when uniaxial traction is applied in the fibres longitudinal direction, both by obtaining the stress-strain curves and by observing the stress distribution. The main focus is to study what are the mechanical factors needed for the achievement of pseudo-ductility.

For that matter the use of a representative volume element with random distribution of fibres is essential and so a simple algorithm to obtain these kind of geometries will be developed with the concern of permitting more than one fibre type/radius. The effect of the variation of fibre arrangements on the RVE equivalent properties will also be a research topic, with the help of the computational programs developed by Guedes and Kikuchi [8] for the implementation of the homogenization theory and the calculation of stress distribution in the microstructure.

The comprehension of the fibrous materials behaviour considering the stochastic values for fibre tensile strength is also a challenge that will be addressed. Using the models presented above, this work results might serve to validate and test optimal solutions for pseudo-ductility provided by simpler models of composite behaviour prediction.

2. RVE Geometry Development

In this chapter it will be presented the MATLAB® script developed for the generation of the RVE geometry of randomly distributed fibres using an optimization approach with a genetic algorithm (GA). The idea is to create a simpler and equally efficient model comparing to those already found in literature, by taking advantage of MATLAB® optimization toolbox.

2.1. Background

Several methodologies in the literature provide random point distributions for a given area, which can be applied in the representative volume element design. The Poisson point pattern provides a basis for random point distributions, and hard-core models treat the points as the centres of the fibres [9]. Digital image analysis was used by Yang et al. [10] to replicate real fibre arrangements by obtaining several microscopic images of the materials analysed. Wongsto and Li's [1] method consist in the perturbation of an hexagonally periodic fibre distribution to generate the transverse randomness of reinforcement. Finally, Melro [11] developed a three-step procedure for generation of random fibre distribution, which includes an hard-core model (initial generation of fibres) and two heuristics, one consisting on stirring the fibres and the other affecting the fibres in the outskirts. This last algorithm is able to generate random distributions for high values of fibre volume fractions.

2.2. Genetic algorithms in optimization

Genetic algorithms are based on Darwin's theory of natural selection. The basic idea of the approach is to start with a set of designs, called the population, by randomly generating N_p genetic strings, or chromosomes, where N_p represents the population size. Each design is assigned a fitness value regarding the cost function. The objective of the GA is to generate a new set of designs from the current set such that the average fitness of the population is improved. The process is continued until a stopping criterion is satisfied or the number of iterations exceeds a specified limit. Three genetic operators are used to accomplish this task: reproduction, crossover, and mutation.

2.3. Model development

The idea behind the developed model is by starting with a random distribution of points, assign radial dimensions to these points and try to separate the circles that are overlapping with others. This is equivalent to stating that we want to minimize the overlapping distances f (Fig. 2(a)). For two fibres

with radius R_1 and R_2,

$$f = \begin{cases} R_1 + R_2 - d, & \text{if } d < R_1 + R_2. \\ 0, & \text{otherwise.} \end{cases} \quad (1)$$

where d represents the distance between the two fibres. If we consider the coordinate system of Fig. 2(b) the distance is then a function of the coordinates (x, y) of each fibre. The assignment of periodic boundary conditions on the generated RVEs when used for FEA also creates dependency from the distance calculations on the dimensions of the microstructure a and b. Thus we can choose the

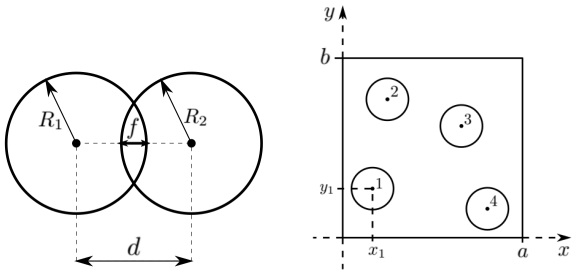

(a) Overlapping distance (b) Coordinate system

Figure 2: Measures of interest.

objective function $F(\mathbf{x}) = \sum f$ being the only design variables $\mathbf{x}$ the coordinates of the fibre centre points. The number of fibres inside the RVE is provided by the required fibre volume fraction as:

$$n_{fibres} = \frac{V_f \times a \times b}{\pi \times R^2} \quad (2)$$

Finally, the formulation for the optimization problem is given by (3).

$$\begin{aligned} \text{minimize} \quad & F(\mathbf{x}, R_i, a, b) \\ \text{w.r.t.} \quad & \mathbf{x} = (x_1, ..., x_{n_{fibres}}, y_1, ..., y_{n_{fibres}}) \\ \text{subject to} \quad & 0 \leq x_i \leq a,\ 0 \leq y_i \leq b, \\ & \text{for } i = 1, ..., n_{fibres} \end{aligned} \quad (3)$$

If no overlapping is found, we get the minimum function value $\min(F) = 0$ and the GA reaches its stopping criterion. The model implemented with the script `randgenGA` uses the `ga` MATLAB® function to minimize the objective function F.

2.4. Implementation

The model is of simple implementation. The input variables include the fibre radius R, the size parameter δ, from where we get the dimensions $a = b = \delta \times R$, the minimum distance parameter Δ_{min} to avoid tangent circles and the required volume fraction V_f. With the input variables chosen, the number of fibres is calculated and then the optimization is performed. After that, there is the generation of new circles to ensure geometric continuity, which consists in replicating the circles that cross the RVE borders or one of its corners in the opposite side or in the remaining corners. The output matrix p contains the information for each circle i: coordinates x_i, y_i, radius R_i (radius varies for the hybrid configuration) and a fourth information specifying which fibre the circle represents (there are more circles than fibres if the circles cross the RVE boundaries dividing the fibres).

2.5. Examples

The method was able to achieve geometries for high fibre volume fraction required for both non-hybrid (one fibre type/radius) and hybrid configuration (two fibre types/radius). An example of a generated geometry for $V_f = 60\% = 30\% + 30\%$ for an hybrid configuration is shown in Fig. 3.

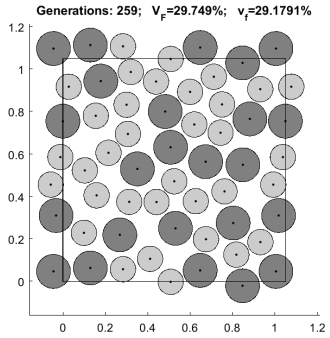

Figure 3: Hybrid configuration with $V_f = 60\%$

The statistical characterisation of the model showed that it is more time consuming than the one generated by Melro [11] but has similar values for the coefficient of variation of the Voronoi polygonal areas and neighbouring distances. Unlike the performance of Melro's [11] algorithm that denoted some flaws for the hybrid configuration considering high fibre volume fractions, the new code developed did not suffer from varying the fibre radius.

3. Equivalent properties

This Chapter aims to present how the mesh is created for FEA and the software needed to compute the homogenized properties of the generated RVE geometries. The homogenization theory is implemented using PREMAT, software developed by Guedes and Kikuchi [8], which uses FEM to compute the material equivalent properties. Thus, the fibre random distributions found with `randgenGA` must be transformed into finite element 3D grids. The grid generation will be conducted in the open-source software Gmsh created by Geuzaine and Remacle [12].

3.1. Homogenization theory

The homogenization theory and its applications are deeply described in the literature [8].
Due to material heterogeneity created by the presence of matrix and fibres, it is extremely difficult to analyse composites at one structural-material level due to the extraordinarily fine discretization required. To overcome this difficulty, one looks for an equivalent material model capable to characterize the average mechanical behaviour as well as represent the effect of the composite material heterogeneities, without representing each individual microstructure.
The homogenization method considers that the composite material is locally formed by the spatial repetition of very small base cells and that if load and boundary conditions are applied to the macrostructure, the resulting deformation and stresses will rapidly vary from point to point because of the repetition of microscopic base cells producing heterogeneity. Thus, all quantities depend on both the macroscopic and microscopic levels, being this last one periodic.
Hence, the local solutions for the microdeformations can be assumed as an asymptotic expansion from where the homogenized material constants can be predicted by applying the problem in the different loading directions.

3.2. Implementation in PREMAT

Following the theory, PREMAT simulates the loading of the RVE in the six tensile and shear directions and computes the stiffness matrix for the homogenized material from the microdeformations obtained for each condition.
To generate the FE mesh the fact that Gmsh has the possibility to generate CAD models by text files with its own scripting language was of much use when designing the mesh from the circle distributions generated by `randgenGA`. The mesh generated will be initially a 2D mesh representing the transverse section obtained. The 2D mesh is generated using a element size parameter `lc` that provides uniform node distances along the surfaces although the appearance of randomness in the created grids. This mesh is then extruded to form a thin 3D grid with only one element used in the z direction.
To export the mesh to PREMAT first we need to pass through the meshing module MESH3D where the periodic boundary conditions are assigned to the nodes in opposite sides of the RVE. The Young's moduli and Poisson's ratios are assigned for the constitutive materials of fibres and matrix as they are needed for the homogenization computations. A compatibility check was performed between generated meshes in Gmsh and the ones already contained in PREMAT as the case of Fig. 4. This figure shows the mesh generated in PREMAT and the mesh generated in Gmsh for the same geometry. The differences between the created grids are easily spotted, with Gmsh providing more elements in the matrix part of the RVE. The results for the homogenized constants were studied and provided similar values validating the use of the FE grids created by Gmsh in PREMAT.

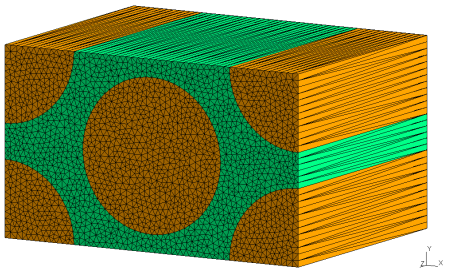

(a) Gmsh

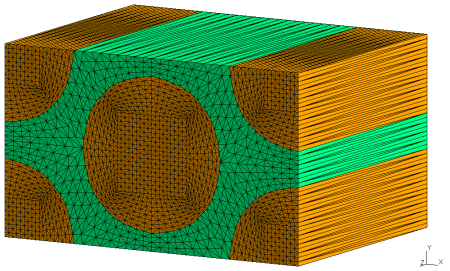

(b) PREMAT

Figure 4: Meshes obtained for RVE type 8.

3.3. Mesh refinement

A study was conducted for the convergence of the homogenized properties to the mesh refinement parameter `lc`. The results for the programs running times, number of elements generated and the average deviation of the diagonal entries of the homogenized constants matrix D from the previous larger value of `lc` are shown in Tab. 1. All runs were performed for the same RVE geometry with random distribution of fibres, for $V_f = 60\%$, $\delta = 15$.

`lc`	Time (s)		Elements	D matrix dev. (%)
	Gmsh	PREMAT		
$a/20$	7.4277	5.6037	2362	-
$a/30$	8.0890	14.6833	3840	1.12
$a/40$	9.8213	30.7623	5648	0.36
$a/50$	15.3999	72.4288	7844	0.52

Table 1: Parametric study for mesh refinement parameter `lc`

We can see that the first value to have a deviation less than 1% from the previous one is `lc`=$a/40$. From there we see that decreasing the element

size leads to more time spending computations, although it does not compensate in the equivalent properties calculated. Therefore, the chosen value for the element size parameter `lc` to use when generating the FE mesh through Gmsh is `lc`=$a/40$.

3.4. Random and regular arrangements

In order to understand how the PREMAT software behaves for RVE geometries created from `randgenGA`, ten tests were conducted with different random fibre distributions and the equivalent properties computed were compared. The runs were made using fibre volume fractions of 50 and 60% and a regular fibre arrangement was taken into account for each one. All tests use the parameters chosen above but the fibres, although with the same properties, were assigned two different radius, as if we were leading with two different materials for the fibres. The resulting data in Tab. 2 correspond to the average number of elements for the ten random distributions obtained, the number of elements obtained for a regular fibre distribution and the deviation of each of the six entries of the diagonal of the homogenized constants matrix D from the ten different random distributions to the ones obtained using the regular distribution, i.e.

$$\sigma(D_{ii_j}) = \frac{D_{ii} - D_{ii_j}}{D_{ii}}, \quad i = 1, ..., 6, \ j = 1, ...10. \tag{4}$$

where D_{ii} are the values for the diagonal entries for a regular distribution and D_{ii_j} are the same values for each of the ten random distributions found. Thereby, the last column represents the average of each of these ten deviations $\bar{\sigma}(D_{ii_j})$ for each diagonal entry of D. Notice that the first three entries of the matrix D diagonal are related to the tensile properties of the composite, respectively E_{11}, E_{22}, E_{33}, and the last three entries represent the shear properties G_{23}, G_{13}, G_{12}[1].

The different transverse section arrangements cause the shear properties to have high deviations, specially those associated with the first and second directions x and y. For the standard values of fibre volume fraction ($V_f = 60\%$), the transverse shear moduli computed show the highest deviations, with regular fibre arrangements providing an overall underestimation of the elastic properties of the material when compared to random packings. This is why it is important to model composite behaviour using transverse randomness of reinforcement, which portrays better the reality of fibre distributions in a composite material.

The values for the number of elements are shown in order to study the response of the FE mesh generator Gmsh to the complex geometries obtained with random distributions. It can be seen that, specially when the fibre volume fraction is high, the number of elements created increases if fibres are randomly arranged in the RVE transverse section. Fig. 5 shows one of the examples analysed for a random distribution and the regular distribution studied for $V_f = 60\%$.

V_f	Elements		$\bar{\sigma}(D_{ii_j})$ (%)
	Random	Regular	
0.5	5338	5236	-7.87 3.12 -0.19 1.90 -14.26 -12.46
0.6	5700	5302	-1.58 -3.29 -0.46 -12.88 -12.01 -33.01

Table 2: Results with regular and random distributions

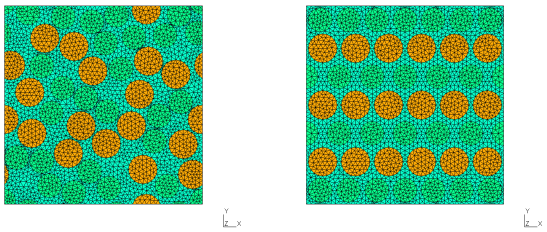

(a) Random distribution (b) Regular distribution

Figure 5: Analysed meshes for $V_f = 60\%$.

4. Damage model

In this chapter the model developed to induce damage on the generated RVE will be presented. The model is a 3D FE model which makes use of POSTMAT [8] program to apply strains and compute the stresses in the microstructure, as a sequence of the computational models developed in the previous chapters.

4.1. Model development

The problem consists in applying uniaxial traction by imposing deformation on the generated 3D RVE in order to plot the stress-strain curve and study the damage on the composite material by the sequential fibre breaking. The primary goal is to model the failure mechanisms of UD composites and to understand how hybridization can change the me-

[1] Note that the longitudinal direction corresponds to the third direction z

chanical behaviour of composite materials, mostly regarding pseudo-ductility.

To compute the strains, displacements and stresses on the RVE, POSTMAT makes use of PREMAT results file `bkaiso.txt` containing the homogenized compliance matrix of the material and the deformation modes utilized in the homogenization computations. The deformation modes `X11, X22, X33, X13, X23, X12` contain the nodal displacements resulting from loading the RVE in each one of these six directions. These local microdeformations will be used in POSTMAT as input, defining the behaviour of the microstructure in each direction. Along with the compliance matrix, by applying strain or stress in one or more chosen directions, POSTMAT is able to compute the nodal strains and stresses in all directions, and with the nodal information, it also computes the information for each element of the mesh.

The deformation is imposed by applying strain in the longitudinal direction of the fibres and the stresses in this direction (z) are computed from this coupling between PREMAT and POSTMAT. POSTMAT results for the stresses in each element of the microstructure are outputted in the file `seqso.txt`. The stress in a single fibre is calculated from a weighted sum of the element stresses corresponding to that fibre. The stress in a fibre f is thus obtained from the following equation:

$$\sigma^f = \frac{\sum V_e^f \sigma_e^f}{\sum V_e^f} \tag{5}$$

where V_e^f and σ_e^f correspond respectively to the volume and stress for an element of the fibre f.

Once the stress in each fibre is calculated, we define the failure criterion for a fibre f:

$$\sigma^f > \sigma_T^f \tag{6}$$

meaning that if the stress computed for a given fibre, σ^f, surpasses the tensile strength assigned for that fibre, σ_T^f, the fibre will be considered broken. The matrix is assumed to have no failure associated throughout the process, meaning that the failure of the composite is controlled solely by fibre breaks.

As the finite element mesh generated considers just one element in length, the failure of a fibre is considered catastrophic for that fibre. The assumption made is that the fibre will continue there, but loose its rigidity. This situation is modelled by reducing the Young modulus of the broken fibre for the subsequent computations.

4.2. Numerical implementation

The numerical implementation was made using MATLAB® script `complete_analysis`, and it is illustrated in Fig. 6. All scripts present in the previous chapters are used along the input variables and parameters studied, including the radius of the fibres, the RVE size parameter δ, the required volume fraction V_f and the element size parameter `lc`. The model starts by running `randgenGA` to generate the RVE cross-section. From the random fibre distribution obtained, the mesh is created and then extruded in Gmsh, to form the 3D finite element grid. The material properties are assigned to fibres and matrix, namely the Young's moduli E_f and E_m and the Poisson's ratios ν_f and ν_m, and then each fibre is given a different tensile strength based on the Weibull distribution [13] for fibre bundles.

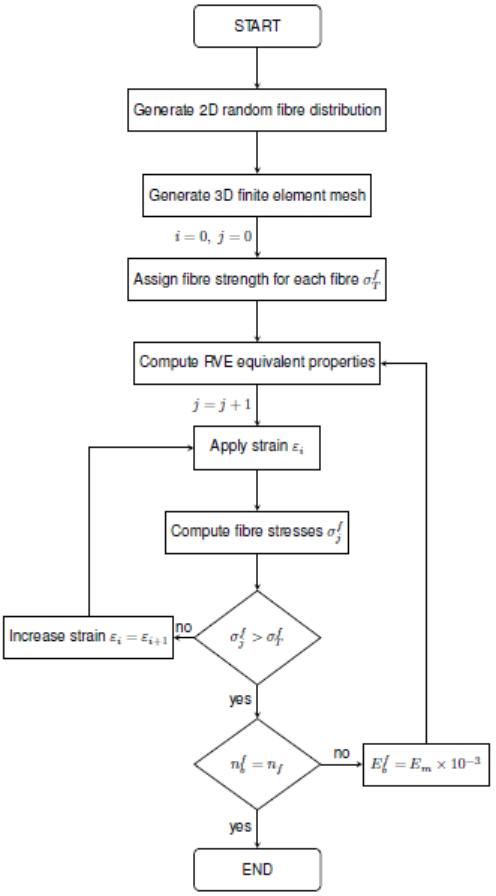

Figure 6: Flowchart for the damage model.

The Weibull probability distribution is given by:

$$P(\sigma) = 1 - exp\left[-\frac{L}{L_0}\left(\frac{\sigma}{\sigma_0}\right)^m\right] \tag{7}$$

where P is the failure probability at the applied stress σ, L is the characteristic gauge length, L_0 is the reference gauge length, σ_0 the scale parameter and m the shape parameter or Weibull modulus [13].

The assignment of the fibre strength for each fibre is done by randomly generating a number $X \in [0, 1]$ that will represent the probability P in Equation

(7), and then the tensile strength for each fibre is calculated from:

$$\sigma_T^f = \sigma_0 \left[-\frac{L_0}{L} ln(1-X) \right]^{\frac{1}{m}} \tag{8}$$

Once the mesh is generated and the fibre tensile strength is assigned, the mesh is exported to PREMAT and the homogenized properties for the RVE are computed, as well as the deformation modes that will be used in POSTMAT.

In the first analysis a small strain ε_0 is applied so that no fibre breaks occur. As long as there are no fibre breaks, we have a linear relation between stress and strain in the composite. Fig. 7 illustrates the predicted behaviour of this model. Note that σ_0 now is not the same of that in Eq. (7) and (8), it corresponds to the stress obtained when a strain ε_0 is applied.

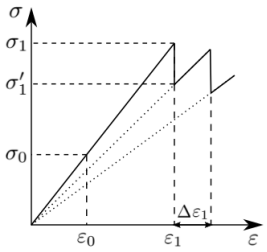

Figure 7: Stress-strain behaviour for the damage model.

As the strain applied is equally distributed along the transverse section, from the POSTMAT result for the stresses on the fibres in this first computation σ_0^f, we assume that there is also a linear proportion between the applied strain and the fibre stresses given by σ_0^f/ε_0. This means that to reach the failure strength σ_T^f for the first fibre we need to take into account the stress in each fibre and with this linear relation find the first strain ε_1 required for a fibre to break:

$$\varepsilon_1 = min \left(\frac{\sigma_T^f}{\sigma_0^f/\varepsilon_0} \right) \tag{9}$$

The resulting stress σ_1^f must meet the failure criterion (6) so that the first fibre breaks. However, underestimations might occur in the strain ε_1 calculated, such that no fibre breaks occur. The solution is to add a very small increment so that the strain applied causes the fibre failure as expected.

When the failure criterion is met, the number of broken fibres n_f^b is updated and the Young's modulus of the broken fibre is reduced to $E_f^b = E_m \times 10^{-3}$. Since this fibre properties were modified, the model will compute the homogenized material constants again in PREMAT and with the same strain compute the stresses for the new homogenized material. This will cause a new value for the linear relation between stress and strain as illustrated by the dotted lines in Fig. 7. In order to achieve a more detailed curve, the next increment of strain will be calculated with the purpose of ensuring that the fibres fail one-by-one:

$$\Delta\varepsilon_i = min \left(\frac{\sigma_T^f - \sigma_i^{f\prime}}{E_f} \right) \tag{10}$$

where i corresponds to the number of broken fibres at some stage of the numerical implementation, i.e $i = 1, ..., n_f$ where n_f is the total number of fibres. The $\sigma_i^{f\prime}$ represents the new stress computed with the same strain applied as given in Fig. 7. Therefore, Eq. (10) means that the next fibre that will break is the one where the most recent computed stress is closer to its tensile strength. The strain in the next computation will be given by:

$$\varepsilon_{i+1} = \varepsilon_i + \Delta\varepsilon_i \tag{11}$$

and applied to the new homogenized material. All strains and average stresses ε_i, σ_i and σ_i' computed for the entire RVE (fibres and matrix) are saved and the process ends with the stress-strain curve response for the composite material plotted when all fibres are broken, i.e. when $n_f^b = n_f$.

5. Results

The damage model will be implemented in microstructures representing carbon fibre reinforced composite materials. The results provided consist in the analysis of the behaviour of two non-hybrid composites and the hybridization considered the two different fibres used. The choice of the materials and parameters of hybridization are based on previous studies developed by Tavares et al. [6]. The influence of considering different tensile strength distributions in the damage model is analysed due to the randomness in the implementation of the Weibull distribution for the fibre bundle.

5.1. Mechanical properties

As stated, two different carbon fibres were chosen with the ultimate goal of creating an hybrid composite capable of representing a pseudo-ductile behaviour. The materials must have different failure strains so that the HE fibres only begin to fail when most of the LE fibres have already failed. The fibre materials that will be utilized in the computations are the AS4 carbon and the M50S carbon, which Weibull parameters and elastic properties are represented in Tab. 3.

For the matrix the assigned properties are those of an epoxy resin with $E_m = 4.6$ GPa and $\nu_m = 0.4$. The Poisson's ratio for the carbon fibres selected is

Mat.	AS4 [14]	M50S [15]
σ_0 (MPa)	4275	4600
L_0 (mm)	12.7	10
m (mm)	10.7	9
E_f (GPa)	234	480
R (μm)	0.35	2.65

Table 3: Mechanical properties for carbon fibres.

a typical value of $\nu_f = 0.35$.
In sequence of the previous chapters, the considered RVEs have side dimensions $a = 15 \times R$ with 1 unit of length in the z direction and the mesh element size parameter `lc`=$a/40$. The values for the gauge length L are neglected by implying $L = L_0$ in the Weibull formula (7).

5.2. Influence of tensile strength distribution
In this section, for the same RVE geometry, five different runs were made with different Weibull distributions for the tensile strength of both AS4 and M50S non-hybrid carbon fibre reinforced composites, with 60% fibre volume fraction. The performance of the different runs is shown in Tab. 4 and 5 and by the stress-strain behaviour in Fig. 8 and 9.

Sim.	ε_1 (%)	σ_{max} (MPa)	ε_f (%)
1	1.38	2114	2.09
2	1.13	2014	2.07
3	1.25	1938	2.04
4	1.07	1952	2.08
5	1.26	1923	2.05
Average	1.22	1988.20	2.07
STDV	0.11	70.10	0.02

Table 4: Initial failure strain, maximum stress and ultimate failure strain for different AS4 fibre strength distributions.

Sim.	ε_1 (%)	σ_{max} (MPa)	ε_f (%)
1	0.59	2102	1.14
2	0.68	2023	1.16
3	0.57	1975	1.08
4	0.53	1868	1.06
5	0.69	2148	1.12
Average	0.61	2023	1.11
STDV	0.07	109.77	0.04

Table 5: Initial failure strain, maximum stress and ultimate failure strain for different M50S fibre strength distributions.

Looking either to the standard deviations tabled either to the stress-strain behaviour of both composites we can perceive that varying the fibre strength distribution has a big influence in the results. It

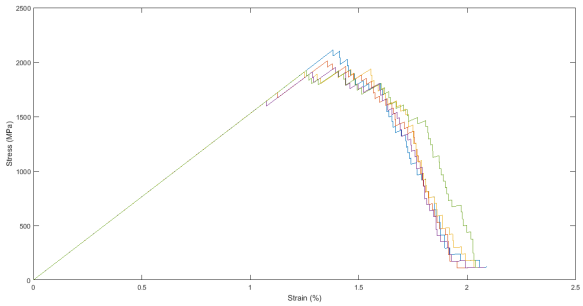

Figure 8: Stress-strain behaviour of AS4 composite for different tensile strength distributions.

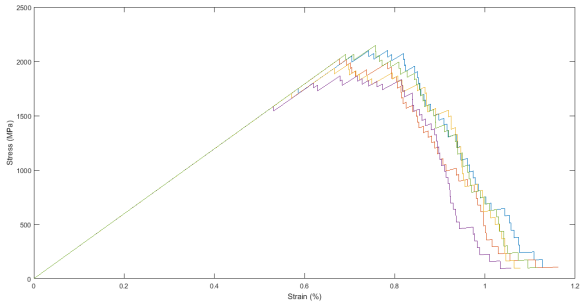

Figure 9: Stress-strain behaviour of M50S composite for different tensile strength distributions.

can be seen that the values for the initial failure strain have the most significant variation for both fibre types.
From the results it is clear which fibre type will be the LE fibre and which will be the HE fibre for hybridization, as the failure strains for the M50S fibre reinforced composite have much lower values than those obtained with AS4 reinforcement.

5.3. Carbon-carbon hybridization
Based on the prediction of the spring element model in [6], the hybrid volume fraction of HE fibres AS4 used is 80%, with 20% of LE fibre M50S content.
First, we study again how different fibre strength distributions might change the composite behaviour, with the mesh obtained for the hybrid RVE illustrated in Fig. 10. The results are tabled in Tab. 6 and plotted in Fig. 11.
It is again important to observe how the initial failure strain varies for the diverse distributions of strength. From the stress-strain behaviour in Figure 11, it can be seen that the tensile strength distribution affects a lot the quest for pseudo-ductility. While the curve in red demonstrates a standard hybrid composite behaviour, the blue curve represents a closer pseudo-ductile response.
For a better comprehension of the hybrid effect, the stress-strain curves are plotted simultaneously in

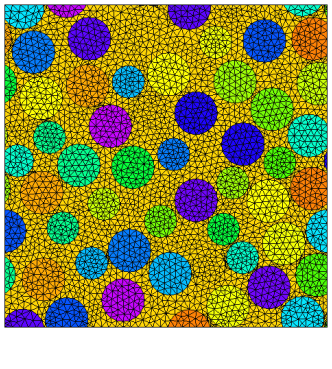

Figure 10: Mesh obtained for hybridization with 80% AS4, 20% M50S.

Sim.	ε_1 (%)	σ_{max} (MPa)	ε_f (%)
1	0.57	1435	2.11
2	0.70	1697	2.03
3	0.80	1597	2.05
4	0.40	1439	2.08
5	0.53	1652	2.02
Average	0.60	1564	2.06
STDV	0.15	121.23	0.04

Table 6: Initial failure strain, maximum stress and ultimate failure strain for different AS4-M50S hybrid fibre strength distributions.

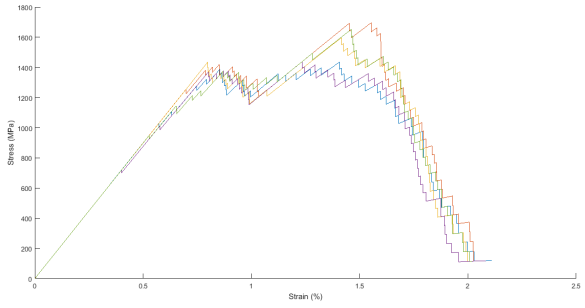

Figure 11: Stress-strain behaviour of hybrid AS4-M50S composite for different tensile strength distributions.

Figure 12 for an all AS4 fibre and an all M50S reinforced non-hybrid composite, along with the configuration studied for the hybridization.

Along with the values obtained in Tab. 6 we observe how the initial failure strain corresponds to the initial failure strain of the LE fibre an the ultimate failure strain is similar to that of the HE fibre. The predominance of the HE fibre content is clear by the slope of the stress-strain line before the first peak corresponding to the initial fibre break. From

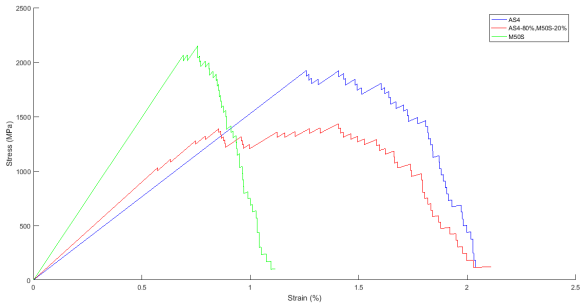

Figure 12: Stress-strain behaviour comparison for AS4 (blue) and M50S (green) non-hybrid composites and AS4-M50S (red) hybrid composite.

there, although not being completely constant, the average stress computed for the composite material microstructure does not face significantly high deviations as the strain increases, having a tendency for the achievement of pseudo-ductility. However, the hybridization causes a clear decrease in the composite strength when compared to both of the non-hybrid behaviours.

6. Conclusions

The first achievement of this work was the successful development of a new methodology to generate transverse randomness of reinforcement. The optimization approach using the genetic algorithm proved to be efficient for high fibre volume fractions, although more time spending compared to the algorithm developed by Melro [11]. For fibre hybrid configurations with two different radius the algorithm had a good performance, and the fact that it can be easily adapted to allow more fibre radius might become useful.

In Chapter 3 the underestimation of the Young and shear moduli for regular fibre packings when compared to random packings [1] was confirmed, proving that for a better micromechanical analysis of composite materials it is important to use random fibre arrangements that portray a closer geometry to the reality of fibrous materials.

The big difference between the damage model implemented and the SEM model [6] is the continuity provided by the 3D finite element mesh with the fibres embedded in the matrix rather than having only one spring element connecting it to a neighbouring fibre. This provides a more complete model with higher complexity and computational effort.

In the hybridization conducted with the two different fibre types AS4 and M50S carbon fibres the choice of the Weibull distribution to assign the tensile strength to the fibres leads to an high variation of the results. Although the pseudo-

ductility is hardly achieved and not for all fibre strength distributions, it is noticeable that there is a tendency for a more ductile behaviour, which could be reached if more fibres were considered. The fact that there are only 15 LE fibres does not allow the best estimations for the overall hybrid composite behaviour, but the estimation achieved closely relates to the ones obtained by Tavares et al. [6] for the SEM model.
An interesting study that could have use with the developed model is the effect of fibre dispersion in hybrid composites. Swolfs et al. [16] made a research explaining how the fibre dispersion can lead to better performances of the hybrid composite. The model was implemented with regular distributions of fibres, thus it would be interesting to use random fibre arrangements and study this dispersion degree which creates a pseudo-ductile behaviour.

Acknowledgements
The author would like to thank Prof. José Miranda Guedes and Prof. Hélder Carriço Rodrigues for the orientation and to Dr. António Melro for providing `RAND_uSTRU_GEN` algorithm.

References

[1] A. Wongsto and S. Li. Micromechanical finite element analysis of unidirectional fibre-reinforced composites with fibres distributed at random over the transverse cross-section. *Composites: Part A*, 36(9):1246 – 1266, 2005.

[2] Y. Swolfs, L. Gorbatikh, and I. Verpoest. Fibre hybridisation in polymer composites: A review. *Composites Part A: Applied Science and Manufacturing*, 67:181 – 200, 2014.

[3] A. Turon, J. Costa, P. Maim, D. Trias, and J.A. Mayugo. A progressive damage model for unidirectional fibre-reinforced composites based on fibre fragmentation. part i: Formulation. *Composites Science and Technology*, 65(13):2039 – 2048, 2005.

[4] R.P. Tavares, A.R. Melro, M.A. Bessa, A. Turon, W.K. Liu, and P.P. Camanho. Mechanics of hybrid polymer composites: analytical and computational study. *Computational Mechanics*, 57(3):405–421, Mar 2016.

[5] F.M. Conde, P.G. Coelho, R.P. Tavares, P.P. Camanho, J.M. Guedes, and H.C. Rodrigues. Optimization of hybrid polymer composites under uniaxial traction. *Engineering Computations*, 35:00–00, 02 2018.

[6] R.P. Tavares, F. Otero, A. Turon, and P.P. Camanho. Effective simulation of the mechanics of longitudinal tensile failure of unidirectional polymer composites. *International Journal of Fracture*, 208(1):269–285, Dec 2017.

[7] T. Okabe, H. Sekine, K. Ishii, M. Nishikawa, and N. Takeda. Numerical method for failure simulation of unidirectional fiber-reinforced composites with spring element model. *Composites Science and Technology*, 65(6):921 – 933, 2005.

[8] J.M. Guedes and N. Kikuchi. Preprocessing and postprocessing for materials based on the homogenization method with adaptive finite element methods. *Computer Methods in Applied Mechanics and Engineering*, 83:143–198, 1990.

[9] V.A. Buryachenko, N.J. Pagano, R.Y. Kim, and J.E. Spowart. Quantitative description and numerical simulation of random microstructures of composites and their effective elastic moduli. *International Journal of Solids and Structures*, 40(1):47 – 72, 2003.

[10] S. Yang, A. Tewari, and A.M. Gokhale. Modeling of non-uniform spatial arrangement of fibers in a ceramic matrix composite. *Acta Materialia*, 45(7):3059 – 3069, 1997.

[11] A.R. Melro, P.P. Camanho, and S.T. Pinho. Generation of random distribution of fibres in long-fibre reinforced composites. *Compos Sci Technol*, 68(9):2091–2102, 2008.

[12] C. Geuzaine and J.-F. Remacle. Gmsh: a three-dimensional finite element mesh generator with built-in pre- and post-processing facilities. *International Journal for Numerical Methods in Engineering*, 79(11):1309 – 1331, 2009.

[13] W. Weibull. A statistical distribution function of wide applicability. *Journal of Applied Mechanics - Transactions of the ASME*, 58(7):1001–1010, 1951.

[14] W. A. Curtin and N. Takeda. Tensile strength of fiber-reinforced composites: Ii. application to polymer matrix composites. *Journal of Composite Materials*, 32(22):2060–2081, 1998.

[15] J. Watanabe, F. Tanaka, H. Okuda, and T. Okabe. Tensile strength distribution of carbon fibers at short gauge lengths. *Advanced Composite Materials*, 23(5-6):535–550, 2014.

[16] Y. Swolfs, R.M. McMeeking, I. Verpoest, and L. Gorbatikh. The effect of fibre dispersion on initial failure strain and cluster development in unidirectional carbon/glass hybrid composites. *Composites Part A: Applied Science and Manufacturing*, 69:279 – 287, 2015.